UD-3 defect in 4*H*, 6*H*, and 15*R* SiC: Electronic structure and phonon coupling

Mt. Wagner,* B. Magnusson,† W. M. Chen, and E. Janzén
Dept. of Physics and Measurement Technology, Linköping University, SE-581 83 Linköping, Sweden

(Received 15 April 2002; published 26 September 2002)

The UD-3 photoluminescence (PL) spectrum is observed in high-resistive or semi-insulating bulk 4*H*, 6*H*, and 15*R* SiC. It consists of one no-phonon (NP) line in 4*H* and 6*H* SiC and two NP lines in 15*R* SiC. The line positions are 1.3555 eV in 4*H* SiC, 1.3440 eV in 6*H* SiC and 1.3474 eV (UD-3_L) and 1.3510 eV (UD-3_H) in 15*R* SiC. In PL excitation experiments, an additional set of four lines (UD-3^{I}–UD-3^{IV}) is observed in all three polytypes. The symmetry of the ground state and the excited states involved in these transitions is determined from Zeeman and polarization experiments. The NP line is accompanied by a broad phonon assisted side band. In addition, three sharp transitions UD-3^a, UD-3^b, and UD-3^c and three broader features have been observed. These are assigned to local phonons.

DOI: 10.1103/PhysRevB.66.115204 PACS number(s): 61.72.Ji, 63.20.Pw, 71.55.Cn, 71.70.Ej

I. INTRODUCTION

SiC is an exciting material, not only for device applications, but also for basic defect studies because it exists in numerous polytypes, the most common ones being 3*C*, 4*H*, 6*H*, and 15*R*. Defects can thus be studied in various environments with decreasing symmetry. But even within a crystal containing only one polytype, a given defect can exist in different configurations. This is due to the existence of inequivalent lattice sites in the polytypes with lower symmetry starting from 4*H*.

Both dopants like the nitrogen donor[1] and deep-level defects like transition metals[2–9] or intrinsic defects[10–15] have been studied in SiC by optical, electrical, and magnetic resonance experiments. Many of these defects have unambiguously been identified; others have defied identification in spite of great efforts, e.g., the D_1 (Ref. 16) and D_2 defects.[17]

Many deep-level defects give rise to photoluminescence (PL) and / or absorption lines in the near infrared spectral region. In semi-insulating samples grown by the technique of high temperature chemical vapor deposition (HTCVD), traces of vanadium[5] and chromium[9] are frequently observed in PL, but there is also an additional series of lines labeled UD-1, UD-2, and UD-3.[18] In this paper, we will concentrate on the UD-3 defect.

This defect has a long and controversial history. When it was reported for the first time in 6*H* SiC,[19] it was believed to be a phonon replica of the *a* line in the *abc* defect system (now known to originate from the neutral silicon vacancy) (Ref. 12) due to a sharp local phonon. Its energy difference to the *a* line is approximately 90 meV, therefore, it was denoted as a_{90}. Hagen and Kemenade later proved that the UD-3 luminescence was not related to the *a* line, in their paper it is called spectrum II.[20] Gorban and Slobodyanyuk agreed on this analysis and relabeled the signal in another paper. At the same time, they extended their studies to the 15*R* polytype and found two lines there. The one line in 6*H* SiC was now called f_1, and the two lines in 15*R* SiC were called f_1 and f_2, respectively.[21] In this report, we choose to adopt the most recent name UD-3.[18]

The aim of this work is to provide detailed information about the electronic structure of the UD-3 defect and its coupling to local phonons. On the basis of this, a model for the recombination mechanism is suggested. The observed signals are best explained assuming that an impurity is involved. Possible candidates for this impurity and their relevant charge states are discussed. However, a complex defect, possibly involving an intrinsic defect, cannot be ruled out at this point.

The paper is organized as follows: In Sec. II, experimental details are provided. Then the experimental results [PL, PL excitation (PLE), polarization, and Zeeman measurements] are presented in Sec. III. These results are discussed in Sec. IV and summarized in Sec. V.

II. EXPERIMENTAL DETAILS

Bulk 4*H*, 6*H*, and 15*R* SiC samples grown by the HTCVD technique have been used in this study. Details about this growth technique can be found in Ref. 22. Their thickness varies between 300 μm and 1 mm. All samples were high resistive or semi-insulating.

The PL and magneto-optical experiments were carried out in a 5 T Oxford split coil superconducting magnet with optical access from four sides, in which the temperature can be varied between 1.5 K and room temperature. The excitation sources were an Ar^+ laser tuned to the 351 nm line in PL and a tunable Ti:Sapphire laser in PLE. The resulting signal was spectrally dispersed by a SPEX 1404 monochromator and detected by a silicon avalanche photo diode or a liquid-nitrogen-cooled germanium detector. Both Faraday and Voigt configuration were used in the Zeeman experiments. Some PL spectra were obtained in a Bomem Fourier transform infrared spectrometer. In this case, the 351 nm line of the Ar^+ laser was used for above-band-gap excitation.

III. RESULTS

A. Photoluminescence

Figure 1 shows PL spectra under above bandgap excitation of the UD-3 defect in 4*H*, 6*H*, and 15*R* SiC. This defect gives rise to one no-phonon (NP) line at 1.3555 eV in 4*H* SiC, one line at 1.3440 eV in 6*H* SiC, and two lines at 1.3474 eV (UD-3_L) and 1.3510 eV (UD-3_H) in 15*R* SiC. At

 ©2002 The American Physical Society

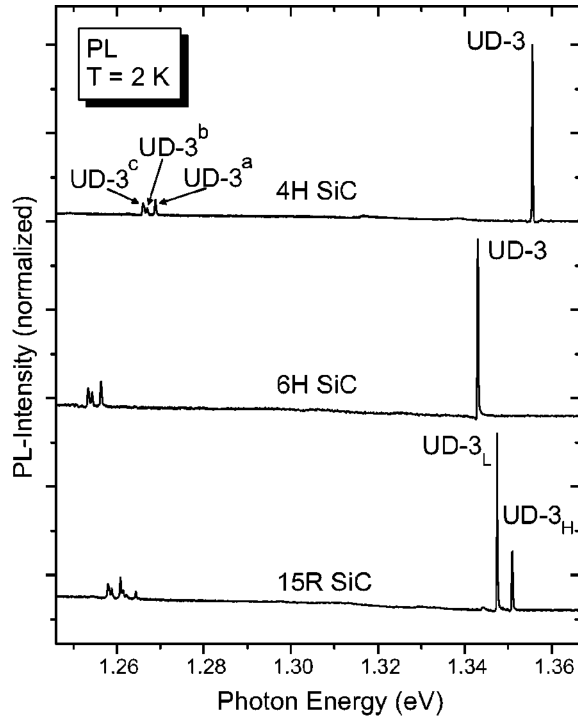

FIG. 1. Photoluminescence (PL) spectra at $T=2$ K of the UD-3 defect in $4H$, $6H$, and $15R$ SiC. There are one no-phonon (NP) line UD-3 in $4H$ and $6H$ SiC and two NP lines UD-3_L and UD-3_H in $15R$ SiC. Each of the NP lines is followed by a broad phonon assisted side band and three sharp transitions UD-3^a, UD-3^b, and UD-3^c, which are attributed to local phonons.

the low-energy side of the NP lines, a broad phonon-assisted side band can be observed together with a series of sharp lines UD-3^a, UD-3^b, and UD-3^c at a distance of approximately 90 meV from the NP line.

In the left part of Fig. 2, results from selective PL (SPL) experiments are shown, in which the excitation energy is fixed to the energy of the UD-3 NP line. Peaks due to the simultaneous emission of two local phonons can be observed (lines UD-3^{a2}–UD-3^{c2}) in addition to UD-3^a–UD-3^c. Beside these, broad phonon replicas are visible at distances of 17–19 and 37–39 meV (depending on the polytype) from UD-3 in both experiments. The energies of all phonons observable are summarized in Table I for all three polytypes.

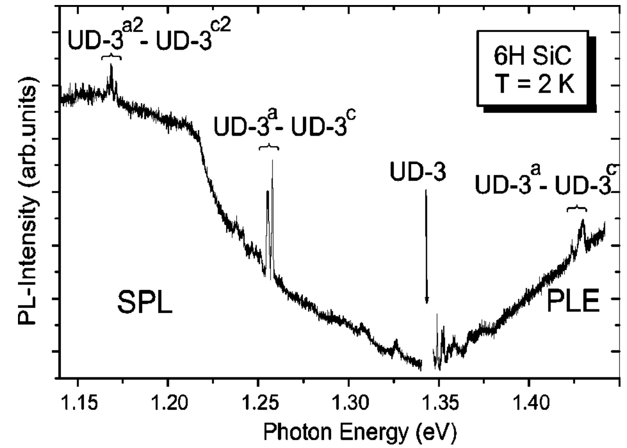

FIG. 2. Selective photoluminescence (SPL) and PL excitation (PLE) spectra at $T=2$ K of the UD-3 defect in $6H$ SiC. In SPL, the exciting laser is tuned to the energy of the NP line UD-3 and the resulting PL is recorded. In PLE, the detection wavelength is fixed to the NP line UD-3 and the excitation wavelength scanned. The local phonons UD-3^a, UD-3^b, and UD-3^c are observed both in SPL and PLE. In SPL, additional features UD-3^{a2}, UD-3^{b2}, and UD-3^{c2} due to the simultaneous emission of two local phonons are visible. The sharp lines close to UD-3 are due to additional excited states (cf. Fig. 4).

There is a remarkable similarity in the phonon energies between the three polytypes.

The phonon-assisted PL band extends toward energies far below UD-3. In Fig. 3, the entire band is shown for the $4H$ polytype in another SPL experiment. Other deep defects like vanadium and chromium can also be excited in a broad range containing the energy of UD-3. In order to separate the contributions of this broad absorption band from the resonant excitation via UD-3, another SPL scan was recorded at an energy slightly lower than UD-3. This spectrum was then subtracted from the UD-3 SPL spectrum. The difference spectrum is displayed in Fig. 3. The peak of the phonon band is located approximately 170 meV below the UD-3 NP line, it has a width of approximately 230 meV.

B. Photoluminescence excitation

When the detection wavelength is fixed to UD-3, it is possible to scan the excitation wavelength, resulting in a

TABLE I. Energies of the local phonons observed in PL and PLE experiments.

Polytype	$4H$ SiC		$6H$ SiC		$15R$ SiC			
NP line (eV)	1.3555		1.3440		1.3474 (UD-3_L)		1.3510 (UD-3_H)	
Experiment	PL	PLE	PL	PLE	PL	PLE	PL	PLE
Phonon replica								
UD-3^a	86.6	78.3	86.6	79.4	86.6	78.8	86.6	79.3
UD-3^b	88.5	82.9	88.7	83.3	88.5	83.1	88.7	83.2
UD-3^c	89.4	85.1	89.5	85.4	89.4	85.2	89.6	85.7
		11.5		11		11		11
	17	16	18	14	18	14	18	16
	39	22	38	22	37	23	37	22

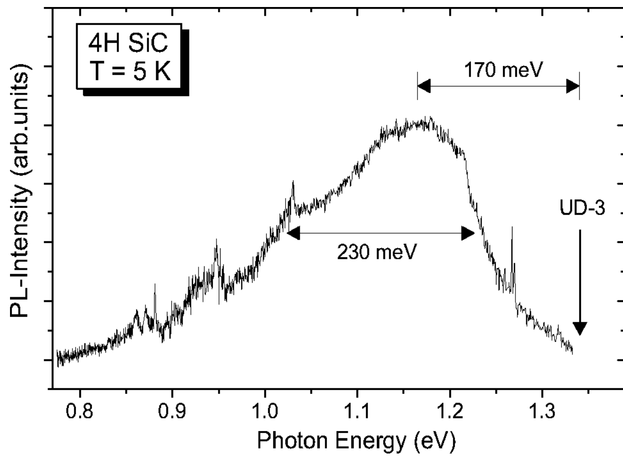

FIG. 3. The phonon assisted side band of the UD-3 defect in 4H SiC at $T=5$ K after subtracting contributions from other defects. The peak of the phonon band is located approximately 170 meV below UD-3, the band has a width of approximately 230 meV.

PLE spectrum. In the right part of Fig. 2, such a PLE spectrum is shown for the 6H polytype together with the results of the SPL experiment. In the PLE scan, a series of sharp transitions only few meV above UD-3 are observed. These lines are discussed below. Other features of the two spectra are remarkably similar. In particular, the sharp lines UD-3^a, UD-3^b, and UD-3^c appear both in SPL and PLE. Therefore, they are attributed to phonon replicas. Their energy does not match any of the known lattice phonons, therefore they are assigned to local phonon modes. The energy distance of these lines from UD-3 is slightly different in SPL compared to PLE, reflecting the fact that these phonon modes have different frequencies depending on whether the defect is in its ground state or in an excited state. Similar to the SPL experiments, there are additional broader phonon replica at energies of 11, 14–16, and 22–23 meV (depending on the polytype) from the NP lines. The energies of all phonon replicas are summarized in Table I.

When the detection energy is fixed to a position deep in the phonon-assisted side band, it is possible to obtain PLE spectra containing even the NP line UD-3. Close ups of the PLE spectra containing UD-3 and the sharp transitions close to it are shown in Fig. 4(a) for the 4H polytype and in Fig. 4(b) for the 6H polytype. Beside the NP line, four additional lines UD-3^{I}–UD-3^{IV} are found. In 15R SiC, the situation is more complicated due to the existence of two NP lines [Fig. 4(c), lower curve]. It is possible to assign the various lines to only one of the NP lines by detecting separately on the NP lines UD-3_{H} and UD-3_{L} and scanning the excitation energy [Fig. 4(c), upper curves]. Again, four additional lines are found for each of the NP lines. In addition, Fig. 4(c) proves that the two NP lines are not connected since it is not possible to excite UD-3_{L} via UD-3_{H}. The line positions of UD-3^{I}–UD-3^{IV} in the three polytypes and their energetic distance to the corresponding NP line are summarized in Table II.

Peaks in a PLE experiment can be due to either higher lying electronic excited states or phonon replicas. Examples of the latter are the lines UD-3^a–UD-3^c. These lines are observable both in PL and PLE experiments at a similar distance to the NP line UD-3. UD-3^{I}–UD-3^{IV}, however, do not have counterparts in PL experiments. It is, therefore, reasonable to assume that they originate from higher lying excited states. Additional evidence for this assignment is obtained from PL experiments at elevated temperatures, where weak hot lines are observable at energies corresponding to

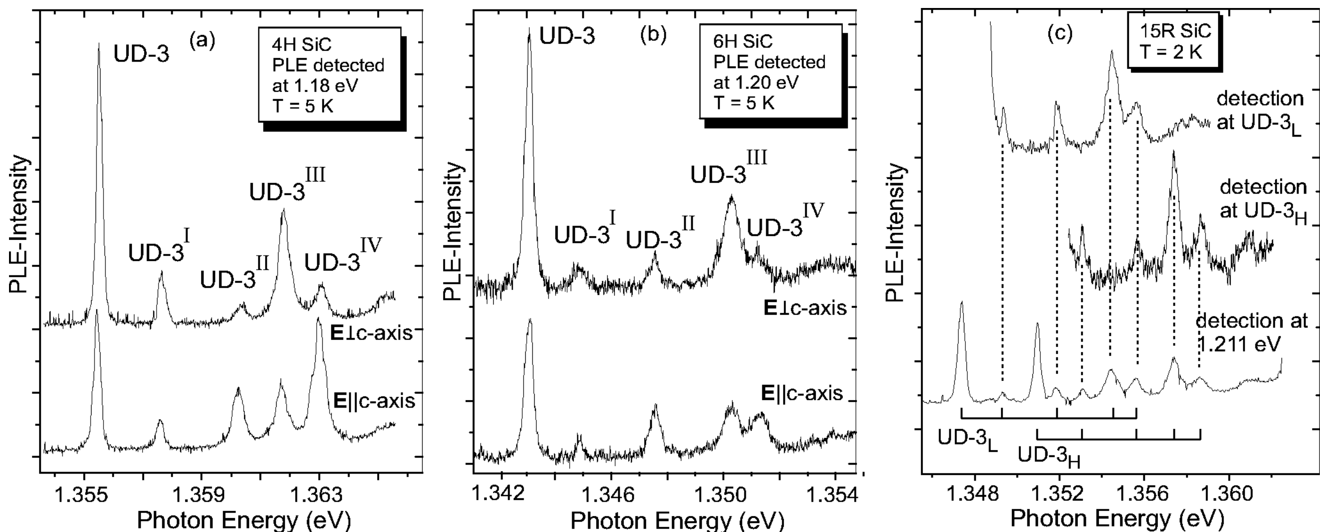

FIG. 4. PLE spectra at $T=5$ K of the UD-3 defect in 4H SiC (a) and 6H SiC (b) detected in the phonon-assisted side band. In the upper spectra, the exciting laser light was polarized $\mathbf{E}\perp c$-axis, in the lower spectra the polarization was $\mathbf{E}\parallel c$-axis. The polarization behavior of the NP line UD-3 and the additional lines due to higher lying excited states UD-3^{I}–UD-3^{IV} is discussed in the text. (c) PLE spectra at $T=2$ K of the UD-3 defect in 15R SiC. The lowest spectrum was detected in the phonon assisted side band. Both NP lines UD-3_{L} and UD-3_{H} are observed, together with several additional excited states. In order to assign the additional lines to either UD-3_{L} or UD-3_{H}, PLE scans were obtained detected at either of the two NP lines (upper spectra). Four lines due to higher lying excited states are observed for both NP lines. UD-3_{L} and UD-3_{H} are not connected since it is impossible to excite UD-3_{L} via UD-3_{H}.

TABLE II. Energetic position and polarization behavior of the NP lines UD-3 and the lines due to the addidtional excited states UD-3^{I}–UD-3^{IV} together with the energetic distance of UD-3^{I}–UD-3^{IV} to the corresponding NP line UD-3.

Line	Energetic position (eV) [Distance to UD-3 (meV)]				Polarization
	$4H$	$6H$	$15R$ (UD-3_L)	$15R$(UD-3_H)	
UD-3	1.3555	1.3440	1.3474	1.3510	$\mathbf{E}\perp c$-axis
UD-3^{I}	1.3576 (2.1)	1.3459 (1.9)	1.3493 (1.9)	1.3530 (2.0)	$\mathbf{E}\parallel c$-axis (weak)
UD-3^{II}	1.3602 (4.7)	1.3485 (4.5)	1.3519 (4.5)	1.3557 (4.7)	$\mathbf{E}\parallel c$-axis
UD-3^{III}	1.3618 (6.3)	1.3513 (7.3)	1.3545 (7.1)	1.3574 (6.4)	$\mathbf{E}\perp c$-axis
UD-3^{IV}	1.3630 (7.5)	1.3523 (8.3)	1.3557 (8.3)	1.3587 (7.7)	$\mathbf{E}\parallel c$-axis

UD-3^{I}–UD-3^{IV} (Fig. 5, $15R$ polytype). The assignment is further supported by the observed variation in polarization within UD-3^{I}–UD-3^{IV} to be discussed below, as phonon replicas should follow the polarization of the associated electronic transition.

C. Polarization and Zeeman experiments

Information about the electronic structure of the levels involved in the optical transitions can be obtained by polarization and Zeeman experiments. Figures 4(a) and 4(b) show PLE spectra of $4H$ SiC and $6H$ SiC with the exciting light polarized both perpendicular (upper curve) and parallel (lower curve) to the c-axis of the crystal. Identical results were obtained for both UD-3_L and UD-3_H in $15R$ SiC. Clearly, the NP line UD-3 and one of the additional lines (UD-3^{III}) are polarized perpendicular to the c-axis, and lines UD-3^{II} and UD-3^{IV} parallel to the c-axis. Line UD-3^{I} exhibits only weak polarization parallel to the c-axis. The results for the NP line UD-3 in $6H$ and $15R$ SiC are consistent with the results previously published.[19] The polarization behavior of all lines is indicated in Table II.

Zeeman experiments can provide additional information about the nature of levels involved in an optical transition. Such experiments were performed both in PL and PLE for all lines in all three polytypes. Each of the NP lines UD-3 splits into two components when the magnetic field is applied parallel to the c-axis. The amount of splitting at $B=5$ T varies among the lines in the different polytypes: 0.59 meV in $4H$ SiC, 0.62 meV in $6H$ SiC, and 0.58 meV (UD-3_L) and

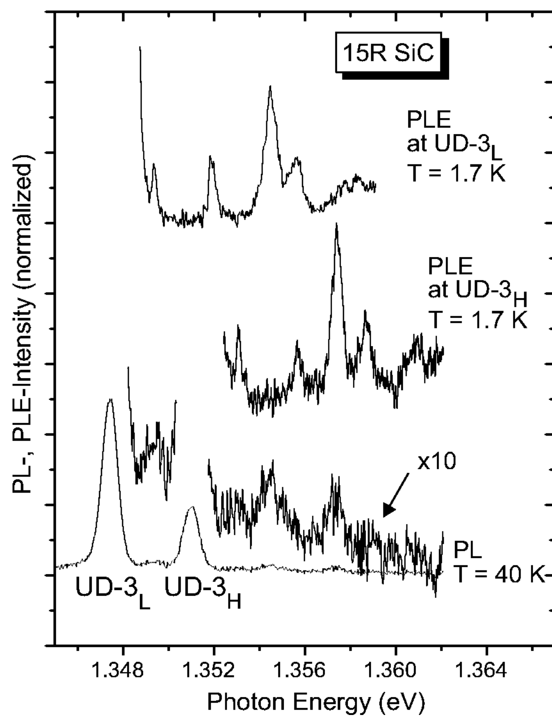

FIG. 5. Photoluminescence of the UD-3 defect in $15R$ SiC at an elevated temperature of $T=40$ K (lowest spectrum). Hot lines appear at positions corresponding to the additional excited states UD-3^{I}–UD-3^{IV} seen in PLE (upper spectra).

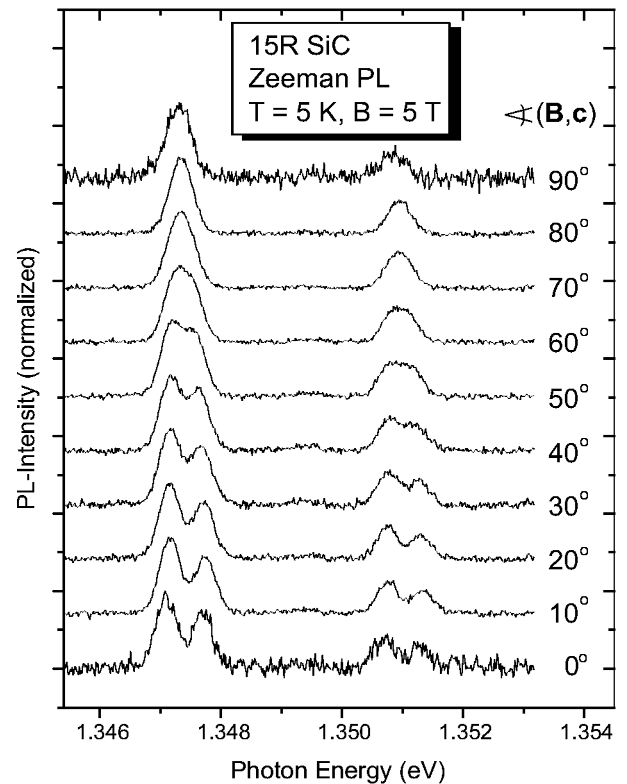

FIG. 6. Zeeman photoluminescence spectra at $T=5$ K and $B=5$ T of the UD-3 defect in $15R$ SiC for various orientations of the magnetic field. 0° corresponds to $\mathbf{B}\parallel c$-axis, and the magnetic field was rotated in the $(\bar{1}100)$-plane. No anisotropy in the basal plane was found.

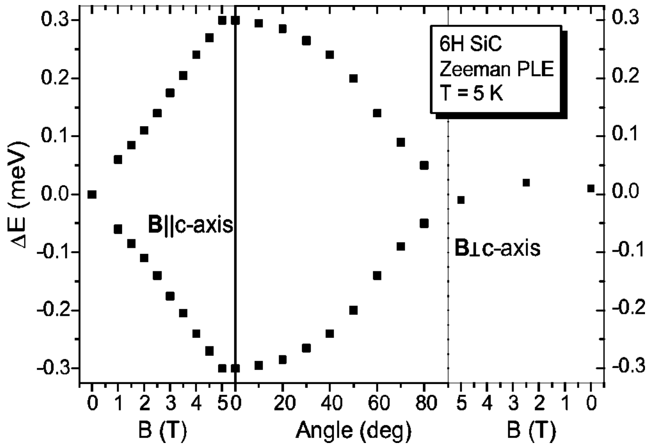

FIG. 7. Magnetic field and angular dependence at $T=5$ K of the Zeeman splitting in PLE experiments for the UD-3 defect in 6H SiC. The splitting is linear in the magnetic field for the $\mathbf{B}\|c$-axis, and the angular dependence is well described by a simple expression for the effective g value: $g_{\mathrm{eff}}=g_{\|}\cos\theta$, $g_{\perp}\approx 0$. No splitting is observed for a magnetic field orientation $\mathbf{B}\perp c$-axis.

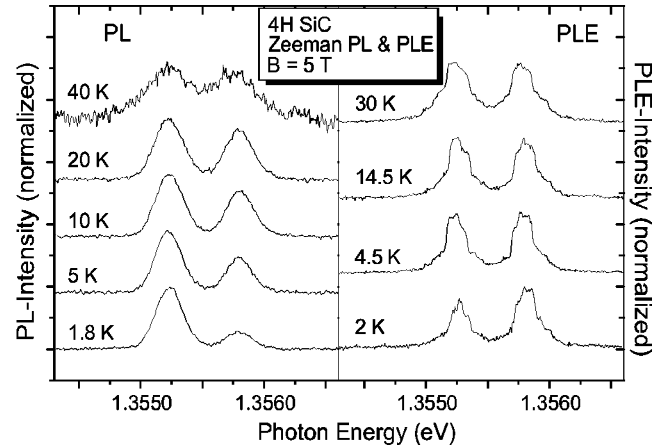

FIG. 8. Zeeman splitting at $B=5$ T in PL and PLE experiments at various temperatures for the UD-3 defect in 4H SiC. In PL, there is a clear thermalization behavior between the two Zeeman components in the temperature range 1.8–40 K. In PLE, the relative intensity of the two components is identical above 4.5 K. At $T=2$ K, the high-energy component is slightly stronger; the reason for this is unclear at the moment.

0.57 meV (UD-3_{H}) in 15R SiC. When the magnetic field $\mathbf{B}$ is rotated away from the c-axis, the splitting decreases and apparently disappears for a magnetic field direction perpendicular to the c-axis (Fig. 6, 15R polytype, lines UD-3_{L} and UD-3_{H}). This is true both for $\mathbf{B}\|[1\bar{1}00]$ and for $\mathbf{B}\|[11\bar{2}0]$. The magnetic field dependent splitting of UD-3 for $\mathbf{B}\|[0001]$ and $\mathbf{B}\|[1\bar{1}00]$ together with an angular dependence at $B=5$ T are displayed in Fig. 7 for the 6H polytype.

Of the additional excited states, only UD-3^{III} was found to be affected by the magnetic field. Due to its large linewidth compared to UD-3 (0.7 meV), the splitting could not be completely resolved at the available maximum field of 5 T. It can, thus, not be determined from these experiments whether the line splits into two or more components. However, the polarization behavior of UD-3^{III} is identical to the one for the NP line UD-3. Furthermore, the splitting disappears when the magnetic field is perpendicular to the c-axis. It is, therefore, plausible to assume that line UD-3^{III} has the same character as the NP line UD-3.

In order to determine whether the splitting occurs in the excited state or the ground state involved in the transition, temperature dependent Zeeman PL and PLE experiments at $B=5$ T were performed (Fig. 8). There is a clear redistribution of intensity in the PL experiments between 1.8 and 40 K, which can be well explained by the assumption of a Boltzmann distribution of carriers between two excited states. No change in relative intensity is observed in PLE between 4.5 and 30 K. At 2 K, the higher energy component is slightly more intense in PLE. The reason for this behavior is unclear at the moment.

IV. DISCUSSION

A. Electronic structure of ground state and excited states

Detailed information about the electronic structure of the ground state and the excited states involved in the optical transition can be extracted from the experimental results. The Zeeman experiments reveal the degeneracy of the levels: In a magnetic field, degenerate levels split into their components according to the effective spin Hamiltonian

$$H=\mu_B\mathbf{S}_{\mathrm{eff}}\cdot\mathbf{g}_{\mathrm{eff}}\cdot\mathbf{B}, \tag{1}$$

with μ_B the Bohr magneton, $\mathbf{S}_{\mathrm{eff}}$ the effective spin, $\mathbf{g}_{\mathrm{eff}}$ the effective g tensor, and $\mathbf{B}$ the magnetic field. The splitting of UD-3 is linear up to the maximum magnetic field of 5 T (Fig. 7). Its angular dependence can be described by a particularly simple expression for the effective g value:

$$g_{\mathrm{eff}}=g_{\|}\cos\theta, \quad g_{\perp}\approx 0. \tag{2}$$

Here θ is the angle between the magnetic field direction and the c-axis of the crystal, $g_{\|}$ the effective g value parallel to the c-axis, and $g_{\perp}$ the effective g value perpendicular to the c-axis. No anisotropy in the basal plane has been found, so the symmetry of the defect is C_{3v} (the symmetry of a substitutional lattice site).

Two Zeeman components are observed at any angle except in perpendicular direction where the two lines coincide. This is true for both PL and PLE experiments at various temperatures. It can, therefore, be concluded that the corresponding transition occurs between a singlet state and a doublet state. Thermalization between the two components is observed in PL experiments, but not in PLE. This implies that it is the excited state, which splits in the magnetic field, whereas the ground state is nondegenerate. In this case, equal intensity in both lines is expected in PLE experiments at any temperature. While this is true above 4.5 K (Fig. 8), there is a minor deviation at 2 K. The reason for this behavior is unclear at this moment. However, a Zeeman splitting of the ground state can be excluded since three of the additional PLE lines (UD-3^{I}, UD-3^{II}, and UD-3^{IV}) do not split in the magnetic field. This implies that they originate from transi-

TABLE III. Effective g values $g_{\parallel}$ of the excited state giving rise to the UD-3 emission for a magnetic field direction parallel to the c-axis ($g_{\perp} \approx 0$ in all cases). The real physical observable $g_{\parallel,L}$ is readily obtained from the effective g value through $g_{\parallel,L} = g_{\parallel}/2$ ($g_{\perp,L} \approx 0$).

Polytype	Line	$g_{\parallel}$	$g_{\parallel,L}$
4H	UD-3	2.04±0.03	1.02±0.03
6H	UD-3	2.14±0.03	1.07±0.03
15R	UD-3_L	2.00±0.03	1.00±0.03
	UD-3_H	1.97±0.03	0.985±0.03

tions between a singlet ground state and singlet excited states. Line UD-3^{III} seems to split in a similar way as the NP line UD-3, although the splitting cannot be completely resolved at the available maximum field of 5 T. The splitting is also largest when the magnetic field is applied parallel to the c-axis, and disappears in perpendicular direction. UD-3^{III} exhibits the same polarization behavior as UD-3; both lines are strongest in $\mathbf{E}\perp c$ polarization. The reverse is true for lines UD-3^{II} and UD-3^{IV}. These lines show $\mathbf{E}\parallel c$ polarization, and they do not split in a magnetic field. Even line UD-3^{I} does not split in the field, but its polarization is only weakly $\mathbf{E}\parallel c$.

The experimental results imply that the ground state of UD-3 is a singlet level. No spin degeneracy was found, so an even number of charge carriers is bound to the defect. The angular dependence of the NP line UD-3 can be explained by assuming an orbital angular momentum $L=1$ for the excited state and no spin degeneracy (i.e., $S=0$). The splitting of such a state in a magnetic field is then described by

$$E(m_l) = g_L \mu_B m_l B. \quad (3)$$

For an unquenched orbital angular momentum and no admixture of higher lying states by spin-orbit interaction, $g_L = 1$. The $m_l=0$ level is split off in the low-symmetry (C_{3v}) crystal field, the $m_l=\pm 1$ levels can then be treated as a doublet in the framework of an effective spin Hamiltonian. An effective spin $S_{\mathrm{eff}}=1/2$ has to be assigned. In Sec. III C it was shown that the splitting of UD-3 in a field of $B=5$ T is approximately 0.6 meV. Using Eq. (1) an effective g-value $g_{\mathrm{eff}} \approx 2$ is obtained readily for $\mathbf{B}\parallel c$-axis. On the other hand, from Eq. (3) the splitting can be calculated as $E(m_l=1) - E(m_l=-1) = 2\mu_B B = 0.579$ meV. The difference can be accounted for by admixture of higher lying excited states through the action of the spin-orbit interaction. The effective g values $g_{\parallel}$ for the magnetic field applied parallel to the c-axis are summarized in Table III. The real physical observable $g_{\parallel,L}$ is readily obtained from the effective g value through $g_{\parallel,L} = g_{\parallel}/2$.

Selection rules for optical transitions apply in a crystal field of symmetry C_{3v}. For an electric dipole transition, the allowed transitions are: $A_1 \leftrightarrow A_2$ and $E \leftrightarrow E$ for $\mathbf{E}\parallel c$ polarization and $A_1 \leftrightarrow E$, $A_2 \leftrightarrow E$, and $E \leftrightarrow E$ for $\mathbf{E}\perp c$ polarization. Experimentally, lines UD-3 and UD-3^{III} were found to be polarized $\mathbf{E}\perp c$, whereas lines UD-3^{II} and UD-3^{IV} show an $\mathbf{E}\parallel c$ polarization. Both the Zeeman results and the polarization behavior of UD-3 and UD-3^{III} can, thus, consistently be

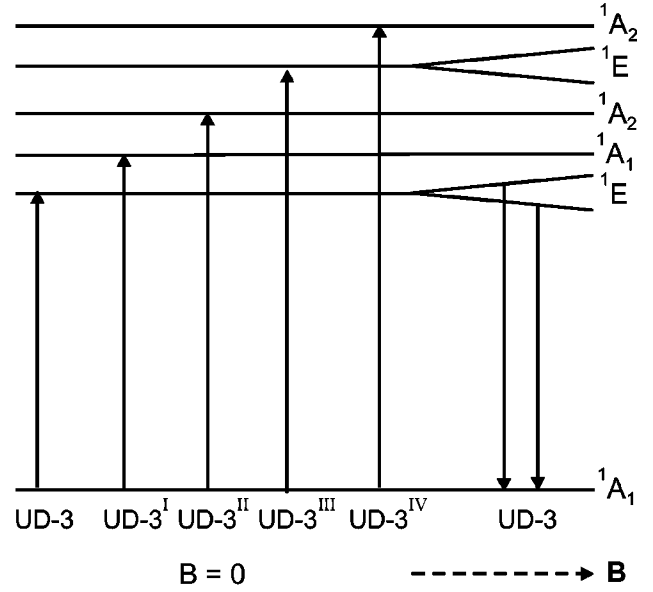

FIG. 9. Schematic of the levels involved in the internal transitions of UD-3. The configuration of the levels in a crystal field of symmetry C_{3v} is indicated.

explained by assuming a transition between a ground state of symmetry A_1 and an excited state of symmetry E. In a similar way, lines UD-3^{II} and UD-3^{IV} can be assigned to transitions $A_1 \leftrightarrow A_2$. Line UD-3^{I} is rather weak and is only weakly polarized $\mathbf{E}\parallel c$. This may imply that this transition occurs between the A_1 ground state and an A_1 excited state. Such a transition is forbidden in both polarizations. However, even the polarization of the other lines is not complete, implying a relaxation of the selection rules. The same relaxation may make line UD-3^{I} slightly allowed and observable.

No spin degeneracy was found in any of the levels involved. Their configurations are therefore deduced to be $^1A_1$ for the ground state and ^1E, $^1A_1$, $^1A_2$, ^1E, and $^1A_2$ for the excited states. A schematic of the levels and the recombination at low temperature is shown in Fig. 9.

B. Recombination mechanism

Radiative transitions in semiconductors at energies far below the band-gap energy, which consist of sharp NP lines, are often due to either recombination of a bound exciton or internal transitions within a deep defect. The observation of a ground state without spin or orbital degeneracy rules out the possibility of an exciton bound to a neutral donor or acceptor because in that case the ground state would be spin degenerate. Even an exciton bound to an isoelectronic impurity can be excluded, since in this case more than two Zeeman components would be expected in a general direction, i.e., when the magnetic field is not parallel to one of the high-symmetry directions. Three or four lines should be observed, depending on whether the orbital angular momentum of the hole is quenched or not.

One possible explanation for the observed Zeeman pattern involves internal transitions of a deep level defect (Fig. 9). This can be either an intrinsic defect like vacancies or anti-

sites, an impurity atom, or complexes of these. Sharp PL lines in the infrared spectral region due to transition metals like vanadium[5] and chromium[9] have been observed in SiC, but also in most other semiconductors. These lines have been attributed to transitions within the $3d$ shell of the atom. Depending on the occupation of the $3d$ shell, various configurations of the ground state and the excited states are possible.

Also some intrinsic defects give rise to internal transitions in the infrared region. Such defects (e.g., vacancies) are likely to be created during the high-temperature growth. Indeed, the well-known PL signal originating from the neutral silicon vacancy[12] can be observed in most of the samples investigated under excitation with the Ti:Sapphire laser.

C. Chemical identity

The phonon replicas found in PL and PLE experiments do not match any of the known lattice phonons in the three polytypes. They are, therefore, attributed to local phonon modes. These modes typically involve vibrations of the impurity atom and one or very few lattice atoms in the close vicinity. Since the nearest neighbor shell of an impurity is almost independent of the polytype (with only minor differences in the distance between neighboring atoms), it is not surprising that these local modes have almost the same energy in all three polytypes. Modes with similar energy compared to the sharp lines between 86.6 and 89.6 meV at the UD-3 defect (Table I) have been found for some transition metal impurities in SiC: titanium in 6*H* SiC with phonon energies 90.1, 89.8, and 89.7 meV,[23] vanadium in 6*H* SiC (89, 88.6, and 88.3 meV; similar values apply for the 4*H* polytype)[5] and chromium (several lines between 85.6 and 88.9 meV in 4*H* and 6*H* SiC).[9]

Recombination at other defects is, in some cases, also accompanied by sharp phonon replicas due to local phonon modes. One example is the D_1 defect, which is presumably of intrinsic nature. However, the energies of the local phonons are in this case found to be 82.7 meV and 83.4 meV,[24] i.e., considerably lower than in UD-3 and the transition metal impurities cited above. Broader features similar to the local phonons in the range 11–39 meV for the UD-3 defect have also been reported in PL spectra of vanadium (22 meV)[5] and titanium (26–30 meV).[3]

For electrons in the *d* shell of a free atom, Hund's rule applies, which states that the spins of all electrons should be aligned parallel, leading to a high-spin configuration of the ground state. The predominantly tetrahedral symmetry (T_d) for a substitutional site in SiC splits the fivefold orbitally degenerate *d* level by the action of the crystal field into a t_{2g} triplet and an e_g doublet, with the triplet lying lower in energy.[25] If the splitting between these two levels is sufficiently large, it becomes energetically favorable to first fill the t_{2g} level, even if this requires violating Hund's rule. Theoretically, a low-spin configuration has been predicted for iron and scandium substituting for a silicon atom in SiC, whereas for the same atoms residing on the carbon sublattice a high-spin configuration is retained.[26] This behavior is explained by the difference in crystal field strength on the two sublattices. In the case of a d^6 configuration, a strong crystal field of symmetry T_d or C_{3v} can lead to a ground state with no spin or orbital degeneracy, i.e., a state with $^1A_1$ symmetry.[27] In order to explain the doublet and singlet nature of the excited states, a crystal field of lower symmetry C_{3v} has to be assumed. It should be mentioned that for a defect residing on an interstitial site, the splitting of the *d*-states will be reversed, the e_g doublet is then lying lower in energy. In this case, a d^4 configuration may explain the $^1A_1$ symmetry of the ground state.

Radiative transitions in the near infrared spectral region due to transition metals of the $3d$ group have been reported before in SiC,[5,9] but also in other semiconductors like GaN.[28,29] As shown above, the energies of the local phonon modes found for the UD-3 defect are very close to the ones reported for Ti, V, and Cr in SiC. These two observations imply that UD-3 may be another impurity of the $3d$ group residing on the same lattice site (the substitutional Si site) since for heavier atoms (like elements from the rare earth group) the phonon energies should be different. An impurity residing on an interstitial site should give rise to completely different phonon modes. A $3d^6$ configuration is possible for Fe^{2+}, Co^{3+}, or Ni^{4+} in free ion notation. The corresponding charge states are $[Fe]^{2-}$, $[Co]^{-}$, and $[Ni]^{0}$. These elements residing on a Si-site are, thus, likely candidates for the UD-3 defect. A direct prove of the chemical identity would be the observation of electron paramagnetic resonance (EPR) or optically detected magnetic resonance (ODMR) signals related to the defect. Unfortunately, the electronic structure of the defect is very unfavorable for such experiments. A splitting of the ground state is necessary for EPR experiments. But as shown by the Zeeman results, the ground state of UD-3 is a spin and orbital singlet. ODMR can be successful if one of the excited states splits in the magnetic field. Even though this is the case for the lowest lying excited state, a microwave induced transition between the $m_l = \pm 1$ states is forbidden. So final defect identification based on such experiments will be difficult.

The investigated samples are all high resistive or semi-insulating. Therefore, the Fermi-level is close to the middle of the band gap. Iron in the negative charge state, i.e., $[Fe]^{-}$, has been observed by EPR in *n*-type 6*H* SiC.[30] If iron does not exhibit a strong negative-*U* behavior, then the doubly negative charge state $[Fe]^{2-}$ can be ruled out for the explanation of UD-3. Not much is known about the electronic structure of cobalt and nickel in SiC. An EPR signal with effective spin $S = 3/2$ in iron-doped SiC, which is observed after illumination with visible or infrared light, has tentatively been assigned to $[Ni]^{-}$ (Ref. 31). However, no hyperfine interaction was observed, therefore other impurities or complexes could not be ruled out. It is interesting to note that in some sublimation grown SiC crystals, iron and nickel were found by secondary ion mass spectroscopy (SIMS) analysis to be major contaminants.[32]

Until the defect has been unambiguously identified (e.g., by intentional doping), alternative defect configurations cannot be ruled out. One possibility would be an intrinsic defect, since internal transitions within such defects can also give rise to luminescence in the infrared spectral region. However, most of the isolated intrinsic defects disappear after

annealing at high temperatures. The UD-3 defect, on the other hand, was found to persist even after an annealing stage at 1625°C for 15 min. Defects of intrinsic nature, which survive up to very high temperatures, have been found in SiC, the most famous one being the D_1 center. Usually, such defects are complex defects like divacancies or vacancy-impurity complexes. The UD-3 defect may have a similar origin. Certain restrictions on the nature of the complex must apply in this case: The defect has a symmetry C_{3v} i.e., the constituents have to be aligned along the *c*-axis.

In many cases, the detailed properties of defects in SiC depend on the inequivalent lattice site on which the defect resides. This is true for shallow dopants like nitrogen,[1] for excitons bound to impurities like titanium,[33] for intrinsic defects like the neutral silicon vacancy,[12] and for internal transitions at transition metal impurities like vanadium[5] and chromium.[9] There are two inequivalent lattice sites in $4H$ SiC, three in $6H$ SiC and five in $15R$ SiC. A corresponding number of distinguishable signals are thus expected for substitutional impurities. There are exceptions from this behavior. The D_1 defect consists of only one NP line in $4H$ SiC,[24] whereas there are three NP lines in $6H$ SiC.[34] For the EPR signal due to the silicon vacancy in the negative charge state only one line has been reported both in $4H$ (Ref. 35) and $6H$ SiC.[11]

The observation of only one NP line due to the UD-3 defect in $4H$ and $6H$ SiC and two NP lines in $15R$ SiC may be explained in several ways. If the defect is a complex, it may contain defects residing on more than one substitutional site. In this case, only one configuration may be possible in $4H$ and $6H$ SiC, while there are two possibilities in $15R$ SiC. For an isolated defect, the energetic position of the corresponding charge state in the band gap may vary between the inequivalent sites. In the case, when either the ground state or the excited state involved in the UD-3 transition is resonant with the valence or conduction band for some inequivalent lattice sites, no radiative recombination via this charge state of the defect will be observable. It is interesting to note that the number of NP lines observed for the UD-3 defect corresponds to the number of *hexagonal* lattice sites in the three polytypes.

V. SUMMARY

The electronic structure of the ground state and the lowest lying excited states of the UD-3 defect in $4H$, $6H$, and $15R$ SiC has been deduced from a combination of PL, PLE, Zeeman, and polarization experiments. From the angular dependence of the Zeeman splitting, the symmetry of the defect is found to be C_{3v}. The ground state is a non-degenerate spin and orbital singlet $^1A_1$, the symmetry of the excited states is ^1E, $^1A_1$, $^1A_2$, ^1E, and $^1A_2$ (in order of increasing energy). This electronic structure implies that the radiative transitions observed are due to internal transitions within a deep-level defect. Besides a broad phonon assisted side band, sharp transitions due to local phonons with energies of approximately 90 meV have been found in PL and PLE experiments.

The energy of the UD-3 luminescence as well as the energy of the local phonons is similar to the ones found for some transition metal impurities like vanadium and chromium in SiC, but also in other semiconductors like GaN. It is therefore possible that the UD-3 defect is another impurity of this kind. A $3d^6$ configuration may explain the singlet electronic structure of the ground state. In this case, $[\mathrm{Fe}]^{2-}$, $[\mathrm{Co}]^{-}$, or $[\mathrm{Ni}]^{0}$ are possible candidates for UD-3. At this point, other defect configurations like a complex defect, possibly involving an intrinsic defect, cannot be ruled out.

ACKNOWLEDGMENTS

The authors would like to thank Okmetic AB for kindly supplying the samples used in this study.

*Email address: matwa@ifm.liu.se

†Also Okmetic AB, SE-583 30 Linköping, Sweden.

[1] H. Woodbury and G. Ludwig, Phys. Rev. **124**, 1083 (1961).

[2] P. J. Dean and R. L. Hartman, Phys. Rev. B **5**, 4911 (1972).

[3] K. M. Lee, L. S. Dang, G. D. Watkins, and W. J. Choyke, Phys. Rev. B **32**, 2273 (1985).

[4] N. Achtziger and W. Witthuhn, Phys. Rev. B **57**, 12 181 (1998).

[5] J. Schneider, H. D. Müller, K. Maier, W. Wilkening, F. Fuchs, A. Dörnen, S. Leibenzeder, and R. Stein, Appl. Phys. Lett. **56**, 1184 (1990).

[6] P. G. Baranov, V. A. Khramtsov, and E. N. Mokhov, Semicond. Sci. Technol. **9**, 1340 (1994).

[7] J. Baur, M. Kunzer, and J. Schneider, Phys. Status Solidi A **162**, 153 (1997).

[8] A. Dörnen, B. Kaufmann, J. Baur, M. Kunzer, J. Schneider, and P. Baranov, in *Proceedings of the 19th International Conference of Defects in Semiconductors. ICDS 19, Aveiro, Portugal, July 1997* [Mater. Sci. Forum **258–263**, 697 (1997)].

[9] N. T. Son, A. Ellison, B. Magnusson, M. F. MacMillan, W. M. Chen, B. Monemar, and E. Janzén, J. Appl. Phys. **86**, 4348 (1999).

[10] H. Itoh, M. Yoshikawa, I. Nashiyama, S. Misawa, H. Okumura, and S. Yoshida, in *Proceedings of the 1990 IEEE Annual Conference on Nuclear and Space Radiation Effects (NSREC), Reno, NV, USA, 16-20 July 1990* [IEEE Trans. Nucl. Sci. **37**, 1732 (1990)].

[11] J. Schneider and K. Maier, in *Proceedings of the 7th Trieste Semiconductor Symposium on Wide Band Gap Semiconductors, Trieste, Italy, 8-12 June 1992* [Physica B **185**, 199 (1993)].

[12] E. Sörman, N. T. Son, W. M. Chen, O. Kordina, C. Hallin, and E. Janzén, Phys. Rev. B **61**, 2613 (2000).

[13] H. J. von Bardeleben, J. L. Cantin, L. Henry, and M. F. Barthe, Phys. Rev. B **62**, 10 841 (2000).

[14] N. T. Son, P. N. Hai, and E. Janzén, Phys. Rev. Lett. **87**, 045502 (2001).

[15] N. T. Son, P. N. Hai, and E. Janzén, Phys. Rev. B **63**, 201201 (2001).

[16] W. J. Choyke and L. Patrick, Phys. Rev. B **4**, 1843 (1971).

[17] L. Patrick and W. J. Choyke, Phys. Rev. B **8**, 1660 (1973).

[18] E. Janzén, A. Henry, J. Bergman, A. Ellison, and B. Magnusson, in *Proceedings of the E-MRS meeting, Strasbourg, France, 2000* [Mater. Sci. Semicond. Proc. **4**, 181 (2001)].

[19] I. S. Gorban and A. V. Slobodyanyuk, Fiz. Tverd. Tela (Leningrad) **15**, 789 (1973) [Sov. Phys. Solid State **15**, 548 (1973)].
[20] S. H. Hagen and A. W. C. van Kemenade, J. Lumin. **9**, 9 (1974).
[21] I. S. Gorban and A. V. Slobodyanyuk, Fiz. Tekh. Poluprovodn. **10**, 1125 (1976) [Sov. Phys. Semicond. **10**, 668 (1976)].
[22] A. Ellison, B. Magnusson, C. Hemmingsson, W. Magnusson, T. Iakimov, L. Storasta, A. Henry, N. Henelius, and E. Janzén, in *Proceedings of the MRS Fall Meeting 2000. Silicon Carbide - Materials, Processing and Devices. Symposium, Boston, MA, USA*, edited by A. Agarwal, M. C. Skowronski, J. A. Carter Jr., and E. Janzén, MRS Symposia Proceedings, No. 640 (Materials Research Society, Warrendale, PA, 2001), H1.2.1.
[23] A. W. C. van Kemenade and S. H. Hagen, Solid State Commun. **14**, 1331 (1974).
[24] T. Egilsson, J. P. Bergman, I. G. Ivanov, A. Henry, and E. Janzén, Phys. Rev. B **59**, 1956 (1999).
[25] Y. Tanabe and S. Sugano, J. Phys. Soc. Jpn. **9**, 753 (1954).
[26] H. Overhof, in *Proceedings of the 23rd International Conference on the Physics of Semiconductors, Berlin, Germany, 21-26 July 1996*, edited by M. Scheffler and R. Zimmermann (World Scientific, Singapore, 1996), p. 2733.
[27] Y. Tanabe and S. Sugano, J. Phys. Soc. Jpn. **9**, 766 (1954).
[28] J. Baur, K. Maier, M. Kunzer, U. Kaufmann, J. Schneider, H. Amano, I. Akasaki, T. Detchprohm, and K. Hiramatsu, Appl. Phys. Lett. **64**, 857 (1994).
[29] R. Heitz, P. Thurian, I. Loa, L. Eckey, A. Hoffmann, I. Broser, K. Pressel, B. K. Meyer, and E. N. Mokhov, Phys. Rev. B **52**, 16 508 (1995).
[30] P. G. Baranov, I. V. Ilyin, E. N. Mokhov, and V. A. Khramtsov, Semicond. Sci. Technol. **16**, 39 (2001).
[31] P. G. Baranov, I. V. Ilyin, E. N. Mokhov, and V. A. Khramtsov, in *Proceedings of the 3rd European Conference on Silicon Carbide and Related Materials, Kloster Banz, Germany, Sept. 2000*, edited by G. Pensl, D. Stephani, and M. Hundhausen (Trans Tech, Uetikon-Zuerich, 2001); Mater. Sci. Forum **353-356**, 529 (2001).
[32] D. Schulz, G. Wagner, J. Dolle, K. Irmscher, T. Müller, H. J. Rost, D. Siche, and J. Wollweber, in *Proceedings of the 12th International Conference on Crystal Growth and the 10th International Conference on Vapor Growth and Epitaxy, Jerusalem, Israel, 26-31 July 1998* [J. Cryst. Growth **198-199**, 1024 (1999)].
[33] L. Patrick and W. J. Choyke, Phys. Rev. B **10**, 5091 (1974).
[34] L. Patrick and W. J. Choyke, Phys. Rev. B **5**, 3253 (1972).
[35] T. Wimbauer, B. K. Meyer, A. Hofstaetter, A. Scharmann, and H. Overhof, Phys. Rev. B **56**, 7384 (1997).